CALCULATION OF THREE-DIMENSIONAL COMPRESSIBLE LAMINAR AND TURBULENT BOUNDARY LAYERS

CALCULATION OF THREE-DIMENSIONAL COMPRESSIBLE BOUNDARY LAYERS ON ARBITRARY WINGS

By Tuncer Cebeci, Kalle Kaups, Judy Ramsey, and Alfred Moser
Douglas Aircraft Company

SUMMARY

A very general method for calculating compressible three-dimensional laminar and turbulent boundary layers on arbitrary wings is described. The method utilizes a non-orthogonal coordinate system for the boundary-layer calculations and includes a geometry package that represents the wing analytically. In the calculations all the geometric parameters of the coordinate system are accounted for. The Reynolds shear-stress terms are modeled by an eddy-viscosity formulation developed by Cebeci. The governing equations are solved by a very efficient two-point finite-difference method used earlier by Keller and Cebeci for two-dimensional flows and later by Cebeci for three-dimensional flows.

Preliminary results for a swept wing look very encouraging. A typical computation time (CPU) for one surface of the wing which roughly consists of 30 z-stations and 20 x-stations with 30 η-points across the boundary layer is a little over 30 sec on an IBM 370/165 computer.

INTRODUCTION

The development of an efficient and accurate method to compute three-dimensional boundary layers on wings of arbitrary shape requires:

(1) The velocity distribution at the boundary-layer edge

(2) A convenient coordinate system

(3) A model for the Reynolds stresses

(4) A numerical method to solve the governing equations

The velocity distribution must be obtained from the pressure distribution. In general, the pressure distribution can be obtained either theoretically or experimentally.

When obtained theoretically, the velocity components in the streamwise and spanwise directions can be calculated without too much difficulty and thus satisfy the first requirement. When the pressure distribution is obtained experimentally, the calculation of the velocity components is rather difficult. Certain approximations must be made to get the velocity distribution from the experimental pressure distribution. In the section "Governing Equations," the difficulties and the procedure used to calculate the velocity components from the experimental pressure distribution are discussed.

In selecting a coordinate system for the boundary-layer calculations, an important point to consider is that the coordinate system should be calculated only once for each geometrical configuration. This rules out the streamline coordinate system since for each angle of attack the streamlines must be calculated repeatedly. Another important point to consider is dictated by utility. The measured or calculated external velocity distributions are usually given in planes containing the local chord line. Hence it is natural to select one surface coordinate in planes parallel to the defining sections. The other surface coordinate may be lines either orthogonal or nonorthogonal to that coordinate line. However, the selection of an orthogonal system causes a number of inconveniences together with lengthy interpolation procedures. As a result, a nonorthogonal coordinate system appears to be the most convenient system with which to perform the boundary-layer calculations as discussed in detail in the section "Coordinate System."

For turbulent flows the governing boundary-layer equations contain the Reynolds stress terms which require closure assumptions such as mixing-length, eddy-viscosity concepts or "higher order turbulence" models. Although the latter have the potential to compute more complicated turbulent flows, mixing-length, eddy-viscosity approaches have proven to yield quite satisfactory results for boundary-layer flows. (See refs. 1 to 4.) The use of higher order turbulence models also increases the complexity of already complex equations leading to high computation times. Furthermore, for compressible flows their accuracy may not be as good as the simple mixing-length, eddy-viscosity methods. For this reason, in our study the Reynolds stresses are modeled by using an accurate eddy-viscosity formulation (see the section "Turbulence Model") developed by Cebeci. (See refs. 3 and 4.)

When physical coordinates are used, the solutions of the governing boundary-layer equations are quite sensitive to the spacings in the streamwise direction (x) and to the spanwise direction (z) and require a large number of x- and z-stations. In calculations such as the ones considered here where the computation time and storage become important, it is necessary to remove the sensitivity to Δx- and Δz-spacings. This can be done by expressing and solving the governing equations in transformed coordinates. Therefore, in the section "Transformation of the Governing Equations," a convenient transformation to express the boundary-layer equations in terms of transformed variables is considered.

In the section "Numerical Method," the solution of the governing equations by the Cebeci-Keller Box method is discussed. This is a very efficient two-point finite-difference method developed by H. B. Keller and applied to the boundary-layer equations by Keller and Cebeci. (See, for example, refs. 5 and 6.)

In the section "Results and Discussion," results for a planar turbulent boundary-layer flow approaching a three-dimensional obstacle and results for a swept wing are presented. Finally in the section "Future Work," additional work that needs to be done in order to develop a complete design tool for computing the flow field past an arbitrary wing is discussed.

SYMBOLS

A	Van Driest damping length, $26(\nu/u_\tau)(\rho/\rho_w)^{1/2}$
b	$= C(1 + \epsilon_m^+)$
C	$= \rho\mu/(\rho_e\mu_e)$
C_p	pressure coefficient, $2(p - p_\infty)/(\rho_\infty u_\infty^2)$
c	the ratio ρ_e/ρ; local chord
c_f	skin-friction coefficient
E	total enthalpy ratio, H/H_e
f	transformed vector potential for ψ
G	$= E'$
g	transformed vector potential for Φ
g'	$= w/w_e$
H	total enthalpy

h, h_1, h_2 metric coefficients

$\vec{i}, \vec{j}, \vec{k}$ unit vectors in $\bar{x}$-, $\bar{y}$-, and $\bar{z}$-directions of Cartesian coordinate system in which wing is defined

$\vec{K}$ curvature vector of coordinate line

$K_1 = K_{g_1}$
$K_2 = K_{g_2}$ } geodesic curvatures

K_{12}, K_{21} geometric parameters

L modified mixing length

M_∞ free-stream Mach number

N_{Pr} Prandtl number

$\vec{n}$ unit vector normal to the surface

P parameter denoting either coordinate, ϕ or $\bar{y}$; point

$P_1, P_2, \ldots, P_{10}$ parameters in transformed differential equations

p static pressure

p_t total pressure

R_e $= u_e s_1 / \nu_e$, Reynolds number

r see figure 7

$\vec{r}$ position vector for point on surface, $(\bar{x}, \bar{y}, \bar{z})$

S stagnation point

s distance along a streamline

s_1	curve length along x-coordinate line
t	time
$\vec{t}$	unit tangent vector along coordinate line
u,v,w,t	dependent variables in first-order, transformed differential equations, f', f'', g', and g''
$\bar{u}$	see figure 7
u_s	total velocity (u_t evaluated at the edge)
u_t	total or resultant velocity
u_τ	friction velocity, $\sqrt{\tau_{t,w}/\rho_w}$
v	velocity normal to surface in physical differential equations
x,z,y	independent coordinates in boundary-layer equations
$\bar{x},\bar{y},\bar{z}$	Cartesian coordinate system used for wing definition
α	local geometric angle of attack of wing section chord lines
β	$= \sin^{-1}(u_p/u_s)$
γ	ratio of specific heats, $\gamma = 1.4$
ϵ(or ϵ_m),ϵ_H	eddy viscosity and eddy conductivity, respectively
η	transformed coordinate normal to surface
θ	angle in tangent plane between x- and z-coordinate lines
λ	local sweep angle, measured between plane normal to free-stream velocity vector and z-coordinate line

μ	molecular viscosity
μ_1,μ_2,μ_3	parameters in transformed energy equation
ν	kinematic viscosity
ρ	density
$\tau_{t,w}$	resultant wall shear stress
τ_x,τ_z	shear stresses
ϕ	stretching variable defined in figure 3
Φ,ψ	two-component vector potentials, equation (56)

Subscripts:

e	outer edge
g	geodesic
I	input stations
i,j,n	indices
in,out	inner and outer regions for eddy viscosity
le	leading edge
p	pivotal points, i.e., stations at which boundary layer is computed
t	wing tip
te	trailing edge
w	wall

∞ free-stream conditions

Primes denote differentiation with respect to η.

GOVERNING EQUATIONS

The governing boundary-layer equations for a nonorthogonal coordinate system are given in references 7 and 8. With a slight change of notation for compressible laminar and turbulent flows, they are given by

Continuity equation:

$$\frac{\partial}{\partial x}(\rho u h_2 \sin\theta) + \frac{\partial}{\partial z}(\rho w h_1 \sin\theta) + \frac{\partial}{\partial y}(\overline{\rho v} h_1 h_2 \sin\theta) = 0 \tag{1}$$

x-momentum equation:

$$\rho \frac{u}{h_1}\frac{\partial u}{\partial x} + \rho \frac{w}{h_2}\frac{\partial u}{\partial z} + \overline{\rho v}\frac{\partial u}{\partial y} - \rho K_1 u^2 \cot\theta + \rho K_2 w^2 \csc\theta + \rho K_{12} uw$$

$$= -\frac{\csc^2\theta}{h_1}\frac{\partial p}{\partial x} + \frac{\cot\theta \csc\theta}{h_2}\frac{\partial p}{\partial z} + \frac{\partial}{\partial y}\left(\mu \frac{\partial u}{\partial y} - \rho\overline{u'v'}\right) \tag{2}$$

z-momentum equation:

$$\rho \frac{u}{h_1}\frac{\partial w}{\partial x} + \rho \frac{w}{h_2}\frac{\partial w}{\partial z} + \overline{\rho v}\frac{\partial w}{\partial y} - \rho K_2 w^2 \cot\theta + \rho K_1 u^2 \csc\theta + \rho K_{21} uw$$

$$= \frac{\cot\theta \csc\theta}{h_1}\frac{\partial p}{\partial x} - \frac{\csc^2\theta}{h_2}\frac{\partial p}{\partial z} + \frac{\partial}{\partial y}\left(\mu \frac{\partial w}{\partial y} - \rho\overline{w'v'}\right) \tag{3}$$

Energy equation:

$$\rho \frac{u}{h_1}\frac{\partial H}{\partial x} + \rho \frac{w}{h_2}\frac{\partial H}{\partial z} + \overline{\rho v}\frac{\partial H}{\partial y} = \frac{\partial}{\partial y}\left[\frac{\mu}{N_{Pr}}\frac{\partial H}{\partial y} + \mu\left(1 - \frac{1}{N_{Pr}}\right)\frac{\partial}{\partial y}\left(\frac{u_t^2}{2}\right) - \rho\overline{v'H'}\right] \tag{4}$$

where $\overline{\rho v} = \rho v + \overline{\rho' v'}$ and h_1 and h_2 are metric coefficients. The latter are functions of x and z, that is,

$$h_1 = h_1(x,z) \qquad h_2 = h_2(x,z) \tag{5}$$

Also, θ represents the angle between the coordinate lines x and z. For an orthogonal system $\theta = \pi/2$. The parameters K_1 and K_2 are known as the geodesic curvatures of the curves z = Constant and x = Constant, respectively. They are given by

$$K_1 = \frac{1}{h_1 h_2 \sin\theta}\left[\frac{\partial}{\partial x}(h_2 \cos\theta) - \frac{\partial h_1}{\partial z}\right]$$

$$K_2 = \frac{1}{h_1 h_2 \sin\theta}\left[\frac{\partial}{\partial z}(h_1 \cos\theta) - \frac{\partial h_2}{\partial x}\right] \qquad (6)$$

The parameters K_{12} and K_{21} are defined by

$$K_{12} = \frac{1}{\sin\theta}\left[-\left(K_1 + \frac{1}{h_1}\frac{\partial\theta}{\partial x}\right) + \cos\theta\left(K_2 + \frac{1}{h_2}\frac{\partial\theta}{\partial z}\right)\right] \qquad (7a)$$

$$K_{21} = \frac{1}{\sin\theta}\left[-\left(K_2 + \frac{1}{h_2}\frac{\partial\theta}{\partial z}\right) + \cos\theta\left(K_1 + \frac{1}{h_1}\frac{\partial\theta}{\partial x}\right)\right] \qquad (7b)$$

The total velocity within the boundary layer u_t is given by

$$u_t = (u^2 + w^2 + 2uw\cos\theta)^{1/2} \qquad (8)$$

One obvious procedure to calculate the velocity components u_e and w_e from the given pressure distribution is to evaluate equations (2) and (3) at the edge of the boundary layer. This gives

$$\frac{u_e}{h_1}\frac{\partial u_e}{\partial x} + \frac{w_e}{h_2}\frac{\partial u_e}{\partial z} - K_1 u_e^2 \cot\theta + K_2 w_e^2 \csc\theta + K_{12} u_e w_e = -\frac{\csc^2\theta}{h_1\rho_e}\frac{\partial p}{\partial x} + \frac{\cot\theta\csc\theta}{h_2\rho_e}\frac{\partial p}{\partial z} \qquad (9)$$

and

$$\frac{u_e}{h_1}\frac{\partial w_e}{\partial x} + \frac{w_e}{h_2}\frac{\partial w_e}{\partial z} - K_2 w_e^2 \cot\theta + K_1 u_e^2 \csc\theta + K_{21} u_e w_e = \frac{\cot\theta\csc\theta}{h_1\rho_e}\frac{\partial p}{\partial x} - \frac{\csc^2\theta}{h_2\rho_e}\frac{\partial p}{\partial z} \qquad (10)$$

Equations (9) and (10), which may be expressed in the form

$$\frac{u_e}{h_1}\frac{\partial u_e}{\partial x} + \frac{w_e}{h_2}\frac{\partial u_e}{\partial z} = F(u_e, w_e, x, z) \qquad (11)$$

and

$$\frac{u_e}{h_1}\frac{\partial w_e}{\partial x} + \frac{w_e}{h_2}\frac{\partial w_e}{\partial z} = G(u_e, w_e, x, z) \qquad (12)$$

constitute a system of first-order quasi-linear partial differential equations in u_e and w_e. The differential relationships for these variables are

$$du_e = \frac{\partial u_e}{\partial x} dx + \frac{\partial u_e}{\partial z} dz \tag{13}$$

$$dw_e = \frac{\partial w_e}{\partial x} dx + \frac{\partial w_e}{\partial z} dz \tag{14}$$

If we let s denote the distance along a streamline, and u_s the total velocity (u_t evaluated at the edge), that is,

$$u_s = \left(u_e^2 + w_e^2 + 2u_e w_e \cos\theta\right)^{1/2} \tag{15}$$

equations (13) and (14) can be expressed in the form

$$u_s \frac{du_e}{ds} = \frac{u_e}{h_1} \frac{\partial u_e}{\partial x} + \frac{w_e}{h_2} \frac{\partial u_e}{\partial z} \tag{16}$$

and

$$u_s \frac{dw_e}{ds} = \frac{u_e}{h_1} \frac{\partial w_e}{\partial x} + \frac{w_e}{h_2} \frac{\partial w_e}{\partial z} \tag{17}$$

by noting that

$$u_s = \frac{ds}{dt} \qquad u_e = h_1 \frac{dx}{dt} \qquad w_e = h_2 \frac{dz}{dt} \tag{18}$$

Comparison of equations (11) and (12) with equations (16) and (17) gives

$$\frac{du_e}{ds} = \frac{F}{u_s} \qquad \frac{dw_e}{ds} = \frac{G}{u_s} \tag{19}$$

In addition, we have the following relationships

$$\frac{dx}{ds} = \frac{u_e}{h_1 u_s} \qquad \frac{dz}{ds} = \frac{w_e}{h_2 u_s} \tag{20}$$

The system of four first-order differential equations (eqs. (19) and (20)) allows one to calculate the variation of u_e, w_e, x, and z along a streamline. In principle, these equations can be solved as an initial-value problem. However, it can be shown that the system of differential equations (11) and (12) has characteristics which are identical to the inviscid streamlines. As a result, the initial-value problem cannot be started from lines which are streamlines. Thus, with initial points on the stagnation line or in the plane of symmetry, the solution is quite difficult except for the initial lines themselves. To obtain the solutions over the entire surface, the initial values of u_e and w_e must be known along a line which is not a streamline itself. However, this information is not available in general. A satisfactory solution requires considerable study. In this study approximate methods are used. The simple sweep theory is known to give reasonable answers

when applied to regions of high-aspect-ratio wings that are outside the influence of root and tip effects. In the absence of spanwise pressure gradients, this approximation is almost exact. Thus, for weak spanwise pressure gradients, we can obtain the velocity components on the midportion of a swept wing with reasonable accuracy by using the sweep theory. In regions of root and tip influence, the simple sweep theory with a correction to the sweep angle is applied. The procedure is explained below.

Consider the velocity vector in the tangent plane at a point P on the wing. (See fig. 1.) The basic assumption for the simple sweep theory is that the velocity component u_p in the z-direction is given by:

$$u_p = u_\infty \sin \lambda \tag{21}$$

The sweep angle λ represents the angle between the spanwise direction and the z-coordinate line through the point P. The parallelogram addition of vector components yields

$$\frac{u_e}{u_\infty} = \frac{u_s}{u_\infty} \frac{\cos \beta}{\sin \theta} \tag{22}$$

$$\frac{w_e}{u_\infty} = \frac{u_s}{u_\infty} \frac{\sin \beta \sin \theta - \cos \theta \cos \beta}{\sin \theta} \tag{23}$$

where $\sin \beta = \dfrac{u_\infty \sin \lambda}{u_s}$.

Elimination of β from equations (22) and (23) yields

$$\frac{u_e}{u_\infty} = \frac{\sqrt{(u_s/u_\infty)^2 - \sin^2 \lambda}}{\sin \theta} \tag{24}$$

$$\frac{w_e}{u_\infty} = \sin \lambda - \frac{u_e}{u_\infty} \cos \theta \tag{25}$$

The total velocity ratio u_s/u_∞ is calculated from

$$\left(\frac{u_s}{u_\infty}\right)^2 = 1 + \frac{1 - \left[\dfrac{p_{t,1}}{p_{t,2}}\left(1 + \dfrac{\gamma}{2} C_p M_\infty^2\right)\right]^{(\gamma-1)/\gamma}}{\dfrac{(\gamma - 1)M_\infty^2}{2}} \tag{26}$$

with $p_{t,1}$ and $p_{t,2}$ denoting the values of total pressure before and after the shock, respectively, and C_p is the pressure coefficient, $C_p = (p - p_\infty)/(1/2\rho u_\infty^2)$. Equation (26) is valid for an adiabatic flow through a shock wave, but since the total pressure ratio across the shock is seldom known, its effect will be neglected. This approximation

introduces only an error of a few percent into the velocity calculations because the total pressure jump across a swept shock is small even for free-stream Mach numbers approaching unity. The total pressure ratio must also remain close to one for the first-order boundary-layer theory to be valid in front of and behind the shock wave.

Equations (24) to (26) are approximately valid for the root and tip regions if the local sweep angle λ is replaced by an effective sweep angle λ_{eff}

$$\left.\begin{aligned}\lambda_{eff} &= \lambda - F_r\lambda_r \\ \lambda_{eff} &= \lambda - F_t\lambda_t\end{aligned}\right\} \tag{27}$$

where λ_r and λ_t denote the root and tip sweep angle for the given z-coordinate line and F_r and F_t are the spanwise interpolation factors for the root and tip, respectively. These parameters are shown schematically in reference 9 as a function of nondimensional spanwise distance in terms of root or tip chord.

COORDINATE SYSTEM

The wing is defined in the $\bar{x},\bar{y},\bar{z}$ coordinate system. Here, the $\bar{x}$-axis is in the direction of the airplane's longitudinal axis and the $\bar{y}$-axis is in the spanwise direction. It is assumed that the wing is defined by a number of airfoil sections in the planes $\bar{y}$ = Constant, which involve the specification of $\bar{z}_i$ and $\bar{x}_i$ for constant values of $\bar{y}_i$. It is also assumed that the pivotal points along the chordwise direction $(\bar{x}/c)_p$ where c denotes local chord are given, as are the spanwise stations $\bar{y}_p$ where the boundary-layer calculations are to be made. These parameters are shown schematically in figure 2.

The defining airfoils are usually given by n pairs of values of $\bar{x}_i$ and $\bar{z}_i$. But because all aerodynamic data related to airfoils are customarily given in terms of fraction of the total chord c, the input data are converted to an xz-coordinate system (see fig. 3) based on the local chord (maximum length line). The relationships between x, $\bar{x}$, z, and $\bar{z}$ are

$$\frac{x}{c} = \frac{1}{c}\left[\left(\bar{x} - \bar{x}_{le}\right)\cos\alpha - \left(\bar{z} - \bar{z}_{le}\right)\sin\alpha\right] \tag{28}$$

$$\frac{z}{c} = \frac{1}{c}\left[\left(\bar{x} - \bar{x}_{le}\right)\sin\alpha + \left(\bar{z} - \bar{z}_{le}\right)\cos\alpha\right] \tag{29}$$

where

$$c = \left[\left(\bar{x}_{te} - \bar{x}_{le}\right)^2 + \left(\bar{z}_{te} - \bar{z}_{le}\right)^2\right]^{1/2} \tag{30}$$

$$\alpha = -\tan^{-1} \frac{\bar{z}_{le} - \bar{z}_{te}}{\bar{x}_{le} - \bar{x}_{te}} \tag{31}$$

The subscripts le and te refer to the points at the leading and trailing edges. They must be specified.

The curves $\bar{y}_j$ = Constant and the curves connecting the points x/c = Constant on all the defining airfoils form a convenient coordinate system. However, the movement of the stagnation point S with angle of attack gives rise to ambiguity. For example, the same x/c value may correspond to two z/c values on a given section. To avoid this problem, another variable ϕ defined by

$$\frac{x}{c} = \frac{1}{2}(1 - \cos \phi) \tag{32}$$

is introduced. Here, $\phi = 0$ corresponds to the leading edge, $\phi = \pi$ corresponds to the trailing edge. The value of ϕ is positive for the upper surface. On the lower surface ϕ is negative.

Other Possible Coordinate Systems

In this section, other possible coordinate systems are discussed. Because of impracticalities with these systems, the nonorthogonal coordinate system is the most convenient to perform the boundary-layer calculations for wing surfaces.

As pointed out in the Introduction, one surface coordinate must be chosen in planes parallel to the defining sections. Consider an orthogonal system in which the orthogonals are constructed between the intersections of planes parallel to the defining sections and the wing surface. Trial calculations showed that orthogonals started from the wing-root congregate at the leading edge, leaving large portions of the wing uncovered. (See fig. 4.) This is especially true for a wing with a sharp trailing edge. A rounded trailing edge rectifies the situation somewhat but there is still a large area of the wing where the orthogonals are sparse.

The orthogonal coordinate system in figure 4 was constructed with the polar angle $\phi = x_2$ at the root section as the other surface coordinate. As is seen from this figure, there are computational difficulties at the trailing edge. To show this, consider figure 5, in which the surface coordinates x_1 and x_2 are obtained by extending the surface coverage with the dashed lines. Here, AA'' is the stagnation line, AB is the root section, and D is a point on the trailing edge. Starting from the initial lines, the boundary layer can be calculated along the line BC'' including the root chord. However, the point D cannot be obtained in a straightforward manner. This is also true for the rest of the trailing-edge points D', D'', and D'''. Because of the difficulty in calculating these trailing-edge points, the orthogonal coordinate system is not practical.

Another possible coordinate system can be obtained by representing the wing by one or more separate conical surfaces. Figure 6 shows such a representation. Here, the wing panels ABDC and CDFE form two conical surfaces with apexes at P and Q, respectively. The shape of the panel ABDC and the coordinate system in the developed plane are shown in figure 7. The initial lines are AC and AB. Line AC is the stagnation line and AB is the wing-fuselage junction. Calculations can be started at corner A. A linear coordinate transformation can be used to avoid marching into the negative r direction. Such a coordinate system without taking the thickness into account (this amounts to representing wing sections by flat plates) was used by Nash and Scruggs (ref. 10). The disadvantage of this coordinate system is the difficulty of doing calculations in the overlap region.

Present Coordinate System

The most convenient coordinate system on the wing surface and the one used in this study is a nonorthogonal coordinate system given by the lines $\bar{y}$ = Constant and ϕ = Constant. The new independent variables ϕ and $\bar{y}$ are selected to correspond to the independent boundary-layer parameters x and z, respectively, in equations (1) to (4). Before the boundary-layer calculations are performed, it is necessary to decide on the surface locations for which the boundary-layer solutions will be output. The best method is a chordwise point distribution in terms of percent chord. The information can then be converted to give the ϕ_p-values for the pivotal points. As is likely to happen, the points on the wing defining sections will not correspond to the pivotal points for the boundary-layer calculations. Thus interpolation is necessary. At each spanwise defining station, the ϕ_I corresponding to the input data can be found by using equations (28) to (32). Next, $\bar{x}_I$ versus ϕ_I and $\bar{z}_I$ versus ϕ_I are curve fitted with cubic spline functions and $\bar{x}_{pI}$ and $\bar{z}_{pI}$ are interpolated for at each spanwise station. Then the $\bar{x}_{pI}$ and $\bar{z}_{pI}$ are spline fitted versus $\bar{y}_j$ for each ϕ_p and are interpolated for $\bar{x}_p$ and $\bar{z}_p$ at $\bar{y}_p$.

Calculation of the Geometric Parameters of the Coordinate System

Once the coordinate system is selected, it is necessary to calculate its geometric parameters, namely, the metric coefficients h_1 and h_2 and K_1 and K_2 which appear in the governing boundary-layer equations. These are calculated by the procedure described below.

The metric coefficient along one curve in space is given by

$$h^2 = \left(\frac{d\bar{x}}{dP}\right)^2 + \left(\frac{d\bar{y}}{dP}\right)^2 + \left(\frac{d\bar{z}}{dP}\right)^2 \tag{33}$$

with P denoting a parameter. For $P = \phi$ along the curves $\bar{y}$ = Constant, equation (33) can be written for h_1 as

$$h_1^2 = \left(\frac{\partial \bar{x}}{\partial \phi}\right)_{\bar{y}}^2 + \left(\frac{\partial \bar{z}}{\partial \phi}\right)_{\bar{y}}^2 \tag{34}$$

Similarly, for $P = \bar{y}$ along the curves ϕ = Constant

$$h_2^2 = 1 + \left(\frac{\partial \bar{x}}{\partial \bar{y}}\right)_{\phi}^2 + \left(\frac{\partial \bar{z}}{\partial \bar{y}}\right)_{\phi}^2 \tag{35}$$

The derivatives in equations (34) and (35), namely $(\partial \bar{x}/\partial \phi)_{\bar{y}}$, $(\partial \bar{z}/\partial \phi)_{\bar{y}}$, $(\partial \bar{x}/\partial \bar{y})_{\phi}$, and $(\partial \bar{z}/\partial \bar{y})_{\phi}$, can be obtained as byproducts of spline-fitting the points along the chordwise and spanwise directions at the pivotal points.

The unit tangent vector $\vec{t}$ along a curve is given by

$$\vec{t} = \frac{d\vec{r}}{ds} = \frac{d\vec{r}}{dP}\frac{1}{ds/dP} = \frac{1}{h}\frac{d\vec{r}}{dP} \tag{36}$$

The unit tangent vector $\vec{t}_1$ along the curve $\bar{y}$ = Constant is

$$\vec{t}_1 = \frac{1}{h_1}\left[\left(\frac{\partial \bar{x}}{\partial \phi}\right)_{\bar{y}}\vec{i} + \left(\frac{\partial \bar{z}}{\partial \phi}\right)_{\bar{y}}\vec{k}\right] \tag{37}$$

where $\vec{i}$, $\vec{j}$, and $\vec{k}$ are unit vectors in the coordinate directions $\bar{x}$, $\bar{y}$, and $\bar{z}$, respectively. The unit tangent vector $\vec{t}_2$ along the curve ϕ = Constant is

$$\vec{t}_2 = \frac{1}{h_2}\left[\left(\frac{\partial \bar{x}}{\partial \bar{y}}\right)_{\phi}\vec{i} + \vec{j} + \left(\frac{\partial \bar{z}}{\partial \bar{y}}\right)_{\phi}\vec{k}\right] \tag{38}$$

The angle between the coordinate lines is then

$$\cos\theta = \vec{t}_1 \cdot \vec{t}_2 = \frac{\left(\frac{\partial \bar{x}}{\partial \phi}\right)\left(\frac{\partial \bar{x}}{\partial \bar{y}}\right) + \left(\frac{\partial \bar{z}}{\partial \phi}\right)\left(\frac{\partial \bar{z}}{\partial \bar{y}}\right)}{h_1 h_2} \tag{39}$$

The curvature of a curve in space is given by

$$\vec{K} = \frac{d\vec{t}}{ds} = \frac{d\vec{t}}{dP}\frac{1}{ds/dP} = \frac{1}{h}\frac{d\vec{t}}{dP} \tag{40}$$

The geodesic or tangential curvature K_g of a curve on the surface can be obtained from

$$K_g = (\vec{t} \times \vec{n}) \cdot \vec{K} \tag{41}$$

Here, $\vec{n}$ is the vector normal to the surface which by definition is

$$\vec{n}\sin\theta = \vec{t}_1 \times \vec{t}_2 \tag{42}$$

or

$$\vec{n} = \frac{1}{h_1 h_2 \sin\theta}\left[-\left(\frac{\partial \bar{z}}{\partial \phi}\right)\vec{i} - \left(\frac{\partial \bar{x}}{\partial \phi}\frac{\partial \bar{z}}{\partial \bar{y}} - \frac{\partial \bar{x}}{\partial \bar{y}}\frac{\partial \bar{z}}{\partial \phi}\right)\vec{j} + \left(\frac{\partial \bar{x}}{\partial \phi}\right)\vec{k}\right] \tag{43}$$

With the use of equation (36), equation (40) can be written as

$$\vec{K} = \frac{1}{h^2}\frac{d^2\vec{r}}{dP^2} - \frac{1}{h^3}\frac{d\vec{r}}{dP}\frac{dh}{dP} = \frac{1}{h^2}\left(\frac{d^2\bar{x}}{dP^2}\vec{i} + \frac{d^2\bar{y}}{dP^2}\vec{j} + \frac{d^2\bar{z}}{dP^2}\vec{k}\right) - \frac{1}{h^4}\left(\frac{d\bar{x}}{dP}\vec{i} + \frac{d\bar{y}}{dP}\vec{j} + \frac{d\bar{z}}{dP}\vec{k}\right)\left(\frac{d^2\bar{x}}{dP^2}\frac{d\bar{x}}{dP}\right.$$

$$\left. + \frac{d^2\bar{y}}{dP^2}\frac{d\bar{y}}{dP} + \frac{d^2\bar{z}}{dP^2}\frac{d\bar{z}}{dP}\right) \tag{44}$$

The geodesic curvature K_{g_1} for a curve $\bar{y}$ = Constant is

$$K_{g_1} = -\left(\vec{t}_1 \times \vec{n}\right) \cdot \vec{K}_1 \tag{45}$$

The minus sign on the right-hand side of equation (45) is introduced to obtain $K_{g_1} = -(1/h_1h_2)(\partial h_1/\partial z)$ in the case of an orthogonal coordinate system. With ϕ as the parameter, the expression for $\vec{K}_1$ is

$$\vec{K}_1 = \frac{1}{h_1{}^2}\left(\frac{\partial^2\bar{x}}{\partial\phi^2}\vec{i} + \frac{\partial^2\bar{z}}{\partial\phi^2}\vec{k}\right) - \frac{1}{h_1{}^4}\left[\left(\frac{\partial\bar{x}}{\partial\phi}\vec{i} + \frac{\partial\bar{z}}{\partial\phi}\vec{k}\right)\left(\frac{\partial^2\bar{x}}{\partial\phi^2}\frac{\partial\bar{x}}{\partial\phi} + \frac{\partial^2\bar{z}}{\partial\phi^2}\frac{\partial\bar{z}}{\partial\phi}\right)\right] \tag{46}$$

Substituting equations (37), (43), and (46) into equation (45) gives, after simplifications

$$K_{g_1} = \frac{1}{h_1{}^4 h_2 \sin\theta}\left(\frac{\partial\bar{x}}{\partial\phi}\frac{\partial\bar{z}}{\partial\bar{y}} - \frac{\partial\bar{x}}{\partial\bar{y}}\frac{\partial\bar{z}}{\partial\phi}\right)\left(\frac{\partial^2\bar{x}}{\partial\phi^2}\frac{\partial\bar{z}}{\partial\phi} - \frac{\partial^2\bar{x}}{\partial\phi^2}\frac{\partial\bar{x}}{\partial\phi}\right) \tag{47}$$

The geodesic curvature K_{g_2} for a curve ϕ = Constant is given by

$$K_{g_2} = \left(\vec{t}_2 \times \vec{n}\right) \cdot \vec{K}_2 \tag{48}$$

With $\bar{y}$ as the parameter, the expression for $\vec{K}_2$ is

$$\vec{K}_2 = \frac{1}{h_2{}^2}\left(\frac{\partial^2\bar{x}}{\partial\bar{y}^2}\vec{i} + \frac{\partial^2\bar{z}}{\partial\bar{y}^2}\vec{k}\right) - \frac{1}{h_2{}^4}\left(\frac{\partial\bar{x}}{\partial\bar{y}}\vec{i} + \vec{j} + \frac{\partial\bar{z}}{\partial\bar{y}}\vec{k}\right)\left(\frac{\partial^2\bar{x}}{\partial\bar{y}^2}\frac{\partial\bar{x}}{\partial\bar{y}} + \frac{\partial^2\bar{z}}{\partial\bar{y}^2}\frac{\partial\bar{z}}{\partial\bar{y}}\right) \tag{49}$$

The expression for the geodesic curvature K_{g_2} is obtained by substitution of equations (38), (43), and (49) into equation (48):

$$K_{g_2} = \frac{1}{h_1 h_2{}^4 \sin\theta}\left[\left(\frac{\partial\bar{x}}{\partial\phi}\frac{\partial\bar{z}}{\partial\bar{y}} - \frac{\partial\bar{x}}{\partial\bar{y}}\frac{\partial\bar{z}}{\partial\phi}\right)\left(\frac{\partial^2\bar{x}}{\partial\bar{y}^2}\frac{\partial\bar{z}}{\partial\bar{y}} - \frac{\partial^2\bar{z}}{\partial\bar{y}^2}\frac{\partial\bar{z}}{\partial\bar{y}}\right) + \left(\frac{\partial^2\bar{x}}{\partial\bar{y}^2}\frac{\partial\bar{x}}{\partial\phi} + \frac{\partial^2\bar{z}}{\partial\bar{y}^2}\frac{\partial\bar{z}}{\partial\phi}\right)\right] \tag{50}$$

The second-order partial derivatives appearing in equations (47) and (50) are also obtained as a byproduct of the spline-fitting technique. In terms of parameters appearing in boundary-layer equations, we set $K_1 = K_{g_1}$ and $K_2 = K_{g_2}$. In addition to θ, h_1, h_2, K_1, and K_2, the boundary-layer equations contain K_{12} and K_{21} which are functions of the previously mentioned parameters. Also, the partial derivatives, $\partial\theta/\partial\phi$ and $\partial\theta/\partial\bar{y}$, are contained in the boundary-layer equations and obtained by spline-fitting θ versus ϕ and $\bar{y}$.

TURBULENCE MODEL

The solution of the system of equations (1) to (4) requires closure assumptions for the Reynolds stresses, $-\rho\overline{u'v'}$, $-\rho\overline{w'v'}$, and $-\rho\overline{v'H'}$. This can be done by a number of approaches. One approach is to use simple eddy-viscosity and mixing-length formulas for the Reynolds stresses. This method, also called the mean-field method, has been used by Cebeci and Smith (ref. 11), Bushnell and Beckwith (ref. 1), and Harris (ref. 2) as well as several others. Another approach is to use expressions that consider the rate of change of the Reynolds stresses in the governing equations. This method, called transport-equation method, has been used by Bradshaw (ref. 12), Donaldson and Sullivan (ref. 13), Hanjalić and Launder (ref. 14), and several others. In reference 15, Bradshaw presents an excellent discussion of both these methods.

For low-speed flows, both approaches work equally well. For high-speed flows, however, the mean-field method seems to be slightly better than the transport-equation method, chiefly because of the inadequate closure assumption accounting for the mean compression or dilatation effect. However, a recent report by Bradshaw (ref. 16) seems to improve substantially the predictions of his method for compressible flows. In either case, equations (1) to (4) are already quite difficult to solve, and there is no need to increase the computation time by using higher order turbulence models. For this reason, an eddy-viscosity formulation developed by Cebeci (refs. 3 and 4) is used in this study. According to this formulation, the boundary layer is divided into two regions, called inner and outer regions, and eddy-viscosity formulas are defined separately in each region.

For a nonorthogonal system (assuming no mass transfer), the inner eddy viscosity is defined by

$$\epsilon_{m,in} = L^2\left[\left(\frac{\partial u}{\partial y}\right)^2 + \left(\frac{\partial w}{\partial y}\right)^2 + 2\cos\theta\left(\frac{\partial u}{\partial y}\right)\left(\frac{\partial w}{\partial y}\right)\right]^{1/2} \tag{51}$$

where

$$L = 0.4y\left[1 - \exp\left(-y/A\right)\right] \tag{52}$$

The total shear stress evaluated at the wall is

$$\tau_{t,w} = \mu\left[\left(\frac{\partial u}{\partial y}\right)_w^2 + \left(\frac{\partial w}{\partial y}\right)_w^2 + 2\cos\theta\left(\frac{\partial u}{\partial y}\right)_w\left(\frac{\partial w}{\partial y}\right)_w\right]^{1/2} \tag{53}$$

The outer eddy viscosity is defined by the formula

$$\epsilon_{m,out} = \alpha\left|\int_0^\infty (u_{t,e} - u_t)dy\right| \tag{54}$$

where

$$u_{t,e} = \left(u_e^2 + w_e^2 + 2u_e w_e \cos\theta\right)^{1/2} \tag{55a}$$

$$u_t = \left(u^2 + w^2 + 2uw\cos\theta\right)^{1/2} \tag{55b}$$

and $\alpha = 0.0168$.

TRANSFORMATION OF THE GOVERNING EQUATIONS

Boundary-Layer Equations

Two-component vector potentials ψ and ϕ are defined such that

$$\left.\begin{aligned} \rho u h_2 \sin\theta &= \frac{\partial\psi}{\partial y} \\ \rho w h_1 \sin\theta &= \frac{\partial\Phi}{\partial y} \\ \overline{\rho v} h_1 h_2 \sin\theta &= -\left(\frac{\partial\psi}{\partial x} + \frac{\partial\Phi}{\partial z}\right) \end{aligned}\right\} \tag{56}$$

The following transformations are also defined

$$x = x \tag{57a}$$

$$z = z \tag{57b}$$

$$d\eta = \left(\frac{u_e}{\rho_e\mu_e s_1}\right)^{1/2}\rho\, dy \tag{57c}$$

$$\psi = \left(\rho_e\mu_e u_e s_1\right)^{1/2} h_2\, f(x,z,\eta)\sin\theta \tag{57d}$$

$$\Phi = \left(\rho_e\mu_e u_e s_1\right)^{1/2}\frac{w_e}{u_e}\, h_1\, g(x,z,\eta)\sin\theta \tag{57e}$$

where

$$s_1 = \int_0^x h_1 \, dx \tag{58}$$

Substituting equations (56) and (57) into equations (2) to (4), after considerable algebra, gives the following:

x-momentum equation:

$$(bf'')' + P_1 ff'' + P_2\left[c - (f')^2\right] + P_5(c - f'g') + P_6 f''g + P_8\left[c - (g')^2\right] = xP_{10}\left[f' \frac{\partial f'}{\partial x} - f'' \frac{\partial f}{\partial x} + P_7\left(g' \frac{\partial f'}{\partial z} - f'' \frac{\partial g}{\partial z}\right)\right] \tag{59}$$

z-momentum equation:

$$(bg'')' + P_1 fg'' + P_4(c - f'g') + P_3\left[c - (g')^2\right] + P_6 gg'' + P_9\left[c - (f')^2\right] = xP_{10}\left[f' \frac{\partial g'}{\partial x} - g'' \frac{\partial f}{\partial x} + P_7\left(g' \frac{\partial g'}{\partial z} - g'' \frac{\partial g}{\partial z}\right)\right] \tag{60}$$

Energy equation:

$$\left(\mu_1 E'\right)' + \mu_2 E' + \mu_3' = xP_{10}\left[f' \frac{\partial E}{\partial x} - E' \frac{\partial f}{\partial x} + P_7\left(g' \frac{\partial E}{\partial z} - E' \frac{\partial g}{\partial z}\right)\right] \tag{61}$$

Here, primes denote differentiation with respect to η and

$$P_1 = \frac{1}{2} + \frac{s_1}{2u_e h_1} \frac{\partial u_e}{\partial x} + \frac{s_1}{2\rho_e \mu_e h_1} \frac{\partial}{\partial x}(\rho_e \mu_e) - s_1\left(K_1 \cot\theta - \frac{K_{12}\cos\theta + K_{21}}{\sin^2\theta}\right) \tag{62a}$$

$$P_2 = \frac{s_1}{u_e h_1} \frac{\partial u_e}{\partial x} - K_1 s_1 \cot\theta \tag{62b}$$

$$P_3 = \frac{s_1}{u_e h_2} \frac{\partial w_e}{\partial z} - K_2 s_1 \frac{w_e}{u_e} \cot\theta \tag{62c}$$

$$P_4 = \frac{s_1}{w_e h_1} \frac{\partial w_e}{\partial x} + K_{21} s_1 \tag{62d}$$

$$P_5 = \frac{w_e}{u_e}\left(K_{12}s_1 + \frac{s_1}{u_e h_2}\frac{\partial u_e}{\partial z}\right) \tag{62e}$$

$$P_6 = \frac{w_e}{u_e}\left[\frac{s_1}{w_e h_2}\frac{\partial w_e}{\partial z} - \frac{s_1}{2u_e h_2}\frac{\partial u_e}{\partial z} + \frac{s_1}{2\rho_e \mu_e h_2}\frac{\partial}{\partial z}(\rho_e \mu_e) + \frac{1}{2h_2}\frac{\partial s_1}{\partial z} - s_1\left(K_2 \cot\theta - \frac{K_{12} + K_{21}\cos\theta}{\sin^2\theta}\right)\right] \tag{62f}$$

$$P_7 = \frac{h_1}{h_2}\frac{w_e}{u_e} \tag{62g}$$

$$P_8 = \left(\frac{w_e}{u_e}\right)^2 K_2 s_1 \csc\theta \tag{62h}$$

$$P_9 = \frac{u_e}{w_e} K_1 s_1 \csc\theta \tag{62i}$$

$$P_{10} = \frac{s_1}{x h_1} \tag{62j}$$

and

$$\mu_1 = C\left(1 + \epsilon^+ \frac{N_{Pr}}{N_{Pr,t}}\right)\frac{1}{N_{Pr}} \tag{63a}$$

$$\mu_2 = P_1 f + P_6 g \tag{63b}$$

$$\mu_3 = C\frac{u_e^2}{H_e}\left(1 - \frac{1}{N_{Pr}}\right)\left[f'f'' + \frac{w_e^2}{u_e^2} g'g'' + \cos\theta \frac{w_e}{u_e}(g'f'' + f'g'')\right] \tag{63c}$$

$$E = \frac{H}{H_e} \tag{63d}$$

$$C = \frac{\rho\mu}{\rho_e \mu_e} \tag{63e}$$

$$b = C(1 + \epsilon_m^+) \tag{63f}$$

$$c = \frac{\rho_e}{\rho} \tag{63g}$$

In the preceding equations, eddy-viscosity and eddy-conductivity concepts have been used in order to satisfy the closure conditions for the Reynolds stresses. They are defined by

$$-\rho\overline{u'v'} = \rho\epsilon_m \frac{\partial u}{\partial y} \qquad -\rho\overline{w'v'} = \rho\epsilon_m \frac{\partial w}{\partial y} \qquad -\rho\overline{v'H'} = \rho\epsilon_H \frac{\partial H}{\partial y} \tag{64}$$

The turbulent Prandtl number $N_{Pr,t}$ and the dimensionless transport coefficients are defined by

$$N_{Pr;t} = \frac{\epsilon_m^+}{\epsilon_H^+} \qquad \epsilon_m^+ = \frac{\epsilon_m}{\nu} \qquad \epsilon^+ = \sqrt{2}\,\epsilon_m^+ \qquad \epsilon_H^+ = \frac{\epsilon_H}{\nu} \tag{65}$$

Equations (59) to (61) are subject to the following boundary conditions:

$$\left.\begin{array}{lllll} \eta = 0 & f = g = 0 & f' = g' = 0 & E' = 0 & \text{(adiabatic wall)} \\ \eta \to \eta_\infty & f' \to 1 & g' \to 1 & E \to 1 & \end{array}\right\} \tag{66}$$

Eddy-Viscosity Equations

The eddy-viscosity formulas given by equations (51) to (55) can also be transformed and expressed as

$$\epsilon_{m,in}^+ = \frac{\mu_e}{\mu}\left[0.4\left(\int_0^\eta \frac{\rho_e}{\rho}\,d\eta\right)\left(1 - e^{-y/A}\right)\frac{\rho}{\rho_e}\right]^2 \left\{R_e\left[(f'')^2 + \frac{w_e}{u_e} g''\left(2f' \cos\theta + \frac{w_e}{u_e} g''\right)\right]\right\}^{1/2} \tag{67}$$

$$\epsilon_{m,out}^+ = 0.0168\left(\frac{\mu_e \rho}{\rho_e \mu}\right)\sqrt{R_e}\left(\int_0^{\eta_\infty} \frac{\rho_e}{\rho}\left\{\left[1 + \frac{w_e}{u_e}\left(2\cos\theta + \frac{w_e}{u_e}\right)\right]^{1/2} - \left[(f')^2 + \frac{w_e}{u_e} g'\left(2f' \cos\theta + \frac{w_e}{u_e} g'\right)\right]^{1/2}\right\} d\eta\right) \tag{68}$$

where

$$\frac{y}{A} = \frac{1}{26}\left(\frac{\mu_w}{\mu_e}\right)^{1/2} R_e^{1/4}\left[\frac{(\rho/\rho_e)^2}{C}\int_0^\eta \frac{\rho_e}{\rho}\,d\eta\right]\left[(f_w'')^2 + \frac{w_e}{u_e} g_w''\left(2f_w' \cos\theta + \frac{w_e}{u_e} g_w''\right)\right]^{1/4} \tag{69}$$

NUMERICAL METHOD

The Cebeci-Keller Box method is used to solve the governing boundary-layer equations given by equations (59) to (61). This is a two-point finite-difference method devel-

oped by H. B. Keller (ref. 17) and applied to the boundary-layer equations by Keller and Cebeci (refs. 5 and 6). The method is discussed in detail in references 6 and 11. For this reason only a brief description will be given here.

One of the basic ideas of this method is to write the governing system of equations in the form of a first-order system. Thus, derivatives of some quantities with respect to the "normal" variable must be introduced as new unknown functions. Derivatives with respect to all other variables occur only to first order as a consequence of the boundary-layer approximations. With the resulting first-order system and an arbitrary rectangular net, centered difference quotients and averages at the midpoints of net rectangles and net segments are used, as required, to get $O(h^2)$ accurate finite-difference equations.

This method is unconditionally stable; however, the equations are highly implicit and nonlinear. Newton's method is employed to solve them. In order to do this with an efficient and stable computational scheme, a block-tridiagonal factorization scheme is used.

Numerical Formulation of the Momentum Equations

New dependent variables $u(x,z,\eta)$, $v(x,z,\eta)$, $w(x,z,\eta)$, and $t(x,z,\eta)$ are introduced, so that equations (59) and (60) can be written as

$$(bv)' + P_1 fv + P_2(c - u^2) + P_5(c - uw) + P_6 gv + P_8(c - w^2) = xP_{10}\left[u\frac{\partial u}{\partial x} - v\frac{\partial f}{\partial x} + P_7\left(w\frac{\partial u}{\partial z} - v\frac{\partial g}{\partial z}\right)\right] \tag{70a}$$

$$(bt)' + P_1 ft + P_4(c - uw) + P_3(c - w^2) + P_6 gt + P_9(c - u^2) = xP_{10}\left[u\frac{\partial w}{\partial x} - t\frac{\partial f}{\partial x} + P_7\left(w\frac{\partial w}{\partial z} - t\frac{\partial g}{\partial z}\right)\right] \tag{70b}$$

$$f' = u \tag{70c}$$

$$u' = v \tag{70d}$$

$$g' = w \tag{70e}$$

$$w' = t \tag{70f}$$

For the net cube shown in figure 8, the net points are

$$x_0 = 0 \qquad x_n = x_{n-1} + k_n \qquad (n = 1, 2, \ldots, N) \tag{71a}$$

$$z_0 = 0 \qquad z_i = z_{i-1} + r_i \qquad (i = 1, 2, \ldots, I) \tag{71b}$$

$$\eta_0 = 0 \qquad \eta_j = \eta_{j-1} + h_j \qquad (j = 1, 2, \ldots, J) \tag{71c}$$

where k_n, r_i, and h_j are defined in figure 8.

The difference equations which are to approximate equations (70c) to (70f) are obtained by averaging about the midpoint $\left(x_{n-\frac{1}{2}}, z_{i-\frac{1}{2}}, \eta_{j-\frac{1}{2}}\right)$

$$\frac{f_j^{n,i} - f_{j-1}^{n,i}}{h_j} = u_{j-\frac{1}{2}}^{n,i} \tag{72a}$$

$$\frac{u_j^{n,i} - u_{j-1}^{n,i}}{h_j} = v_{j-\frac{1}{2}}^{n,i} \tag{72b}$$

$$\frac{g_j^{n,i} - g_{j-1}^{n,i}}{h_j} = w_{j-\frac{1}{2}}^{n,i} \tag{72c}$$

$$\frac{w_j^{n,i} - w_{j-1}^{n,i}}{h_j} = t_{j-\frac{1}{2}}^{n,i} \tag{72d}$$

where, for example,

$$u_{j-\frac{1}{2}}^{n,i} = \frac{1}{2}\left(u_j^{n,i} + u_{j-1}^{n,i}\right)$$

The difference equations used to approximate equations (70a) and (70b) are rather lengthy. To illustrate the difference equations, an example equation similar to equations (70a) and (70b) is chosen as follows:

$$v' + P_1 f v = x\left(u \frac{\partial u}{\partial x} + P_7 w \frac{\partial u}{\partial z}\right) \tag{73}$$

The difference equations for this equation are

$$\frac{\bar{v}_j - \bar{v}_{j-1}}{h_j} + (P_1)_{i-\frac{1}{2}}^{n-\frac{1}{2}} \overline{(fv)}_{j-\frac{1}{2}} = x^{n-\frac{1}{2}}\left[\bar{u}_{j-\frac{1}{2}}\left(\frac{\bar{u}_n - \bar{u}_{n-1}}{k_n}\right) + (P_7)_{i-\frac{1}{2}}^{n-\frac{1}{2}} \bar{w}_{j-\frac{1}{2}}\left(\frac{\bar{u}_i - \bar{u}_{i-1}}{r_i}\right)\right] \tag{74}$$

where, for example,

$$\bar{v}_j = \frac{1}{4}\left(v_j^{n,i} + v_j^{n,i-1} + v_j^{n-1,i-1} + v_j^{n-1,i}\right)$$

$$\bar{u}_n = \frac{1}{4}\left(u_j^{n,i} + u_j^{n,i-1} + u_{j-1}^{n,i} + u_{j-1}^{n,i-1}\right)$$

$$\bar{u}_i = \frac{1}{4}\left(u_j^{n,i} + u_j^{n-1,i} + u_{j-1}^{n,i} + u_{j-1}^{n-1,i}\right)$$

$$P_{i-\frac{1}{2}}^{n-\frac{1}{2}} = \frac{1}{4}\left(P_i^n + P_{i-1}^n + P_i^{n-1} + P_{i-1}^{n-1}\right)$$

The boundary conditions for equations (70) evaluated at $x = x_n$ and at $z = z_i$ are

$$\left.\begin{aligned} f_0^{n,i} &= 0 \qquad g_0^{n,i} = 0 \qquad u_0^{n,i} = 0 \\ w_0^{n,i} &= 0 \qquad u_J^{n,i} = 1 \qquad w_J^{n,i} = 1 \end{aligned}\right\} \tag{75}$$

If $\left(f_j^{n-1,i-1}, u_j^{n-1,i-1}, v_j^{n-1,i-1}, g_j^{n-1,i-1}, w_j^{n-1,i-1}, t_j^{n-1,i-1}\right)$, $\left(f_j^{n,i-1}, u_j^{n,i-1}, v_j^{n,i-1}, g_j^{n,i-1}, w_j^{n,i-1}, t_j^{n,i-1}\right)$, and $\left(f_j^{n-1,i}, u_j^{n-1,i}, v_j^{n-1,i}, g_j^{n-1,i}, w_j^{n-1,i}, t_j^{n-1,i}\right)$ are assumed to be known for $0 \leq j \leq J$, then the difference equations (70a), (70b), (72), and (75) yield an implicit nonlinear algebraic system of $6J + 6$ equations in as many unknowns $\left(f_j^n, u_j^n, v_j^n, g_j^n, w_j^n, t_j^n\right)$. This nonlinear system is solved by means of Newton's method. The resulting linearized system is then solved very efficiently by using the block elimination method discussed by Isaacson and Keller (ref. 18).

Numerical Formulation of the Energy Equation

A new dependent variable $G(x,z,\eta)$ is defined as

$$G = E' \tag{76a}$$

and equation (61) is written as

$$(\mu_1 G)' + \mu_2 G + \mu_3' = xP_{10}\left[u\frac{\partial E}{\partial x} - G\frac{\partial f}{\partial x} + P_7\left(w\frac{\partial E}{\partial z} - G\frac{\partial g}{\partial z}\right)\right] \tag{76b}$$

The difference equation for (76a) is written again by averaging about the midpoint $\left(x_n, z_i, \eta_{j-\frac{1}{2}}\right)$, and is similar to those given by equation (72). The difference equation for equation (76b) is written similar to equation (74). The boundary conditions for an adiabatic wall are

$$G_0^{n,i} = 0 \qquad E_J^{n,i} = 1 \tag{77}$$

The resulting algebraic system of $2J + 2$ equations in as many unknowns $\left(E_j^{n,i}, G_j^{n,i}\right)$, which is linear, is directly solved by the block elimination method.

RESULTS AND DISCUSSION

One obvious difficulty in evaluating the accuracy of the three-dimensional turbulent boundary-layer calculations on wings is the lack of complete, reliable data. Fortunately, however, there are a few good data available for flows with simple geometries. Calculations for these flows serve the useful purpose of evaluating the turbulence models used for the Reynolds stresses. References 3 and 4 present several comparisons of calculations with experimental data. Although these comparisons are for flows over simple geometries and the calculations are for a coordinate system different than the one considered here, the generally good agreement observed in those calculations gives some confidence in the accuracy of the turbulence model used in this study. Figure 9, taken from reference 19, shows the flow geometry and comparisons of calculated and experimental results for a planar turbulent boundary-layer flow approaching a three-dimensional obstacle. The results shown are for velocity profiles in a gradually steepening adverse pressure gradient flow off the plane of symmetry. The calculations were made for a Cartesian coordinate system which can be obtained from the present equations by setting $h_1 = h_2 = 1$, $K_1 = K_2 = K_{12} = K_{21} = 0$, and $\theta = \pi/2$.

Skin-friction coefficients are presented in figure 10 for the upper surface of a swept wing whose planform is given in reference 10. The calculations were made by obtaining the velocity components from the experimental pressure distribution by the procedure discussed earlier. To simulate the actual geometry, a reasonable thickness distribution was added to the planar wing considered in reference 10. As in reference 10, the calculations were made for a unit Reynolds number of 4.92×10^6 per meter and for a free-stream Mach number M_∞ of 0.5. In the figure $z = 1.778$ m represents an inboard station on the wing and $z = 4.572$ m represents a station in the middle of the outboard panel of the wing. The skin-friction coefficients are defined as surface shear-stress components normalized with free-stream dynamic pressure. Here, $c_{f,x}$ represents the shear-stress component in the x-coordinate direction and $c_{f,z}$ represents the shear-stress component normal to the x-coordinate in the tangent plane. In physical and transformed coordinates, they are defined by the following formulas:

$$c_{f,x} = \frac{\tau_x + \tau_z \cos\theta}{\frac{1}{2}\rho_\infty u_\infty^2} = \frac{2C_w}{\sqrt{R_e}}\left(\frac{\rho_e}{\rho_\infty}\right)\left[\left(\frac{u_e}{u_\infty}\right)^2 f_w'' + \frac{u_e w_e}{u_\infty^2} g_w'' \cos\theta\right] \tag{78}$$

$$c_{f,z} = \frac{\tau_z \sin\theta}{\frac{1}{2}\rho_\infty u_\infty^2} = \frac{2C_w}{\sqrt{R_e}}\left(\frac{\rho_e}{\rho_\infty}\right)\frac{u_e w_e}{u_\infty^2} g_w'' \sin\theta \tag{79}$$

Although the present results and those of reference 10 are qualitatively similar, there are several quantitative differences between the two predictions. One possible reason for the differences could be the starting procedure used to compute the initial conditions along the spanwise direction. Our calculations were made for a turbulent flow starting at approximately 3-percent chord whereas the calculations of reference 10 were made with transition to turbulent flow occurring at 10-percent chord. Another possible reason for the differences could be the procedure used to get the velocity components from the experimental pressure distribution.

The method described in the previous section resulted in the three computer programs which are used separately from each other. One computer program deals with the calculation of the velocity components from the experimental pressure distribution by using the sweep theory. Obviously if the velocity components are known from the inviscid flow theory, then this program is not needed. The second computer program deals with the calculation of the nonorthogonal coordinate system and its geometric parameters, namely, the metric coefficients h_1, h_2, K_1, and K_2 appearing in the governing boundary-layer equations. Through the use of this program, the coordinate system and its geometric parameters are calculated once and for all for a given wing. The data is punched out on cards to be stored. If no changes are made in the airfoil cross sections, then this data can be used for any number of boundary-layer calculations without using the second computer program again. The third computer program deals with the solution of the governing boundary-layer equations for a nonorthogonal system using the very efficient and accurate Cebeci-Keller Box method. This program assumes that initial conditions on two intersecting lines are given. In the present program, the two intersecting lines correspond to the wing-fuselage junction and to a line along the span a small fraction of the chord length away from the leading edge. This computer program solves the boundary-layer equations in a surprisingly small amount of time for a given external velocity distribution (either experimental or theoretical) and for a given wing coordinate system for both incompressible and compressible flows. The results in figure 10, for example, were obtained for a wing consisting of 29 z-stations and 19 x-stations with 30 η-points across the boundary layer. The total central-processing-unit (CPU) time for all stations is approximately 30 sec on an IBM 370/165 computer.

FUTURE WORK

The method described here has been tested for only one flow condition. It lacks certain important features and capabilities that may become very useful at different flow conditions, particularly for the third computer program which solves the boundary-layer equations. These features and capabilities conveniently can be divided into three separate tasks.

1. It is desirable and useful to include the capability of starting the calculations at the stagnation line rather than some small distance aft of the stagnation line as in the present procedure. This task involves the solution of a special set of equations, called attachment-line equations. With this capability, the solution of one of the initial lines (stagnation line) becomes exact but remains approximate (though a good approximation) on the other initial line (wing-fuselage juncture) as before.

2. In the present method, the dimensionless cross-flow velocity is defined by $g' = w/w_e$. However, this definition is not very convenient. In some problems where the outer velocity component w_e changes sign, certain ambiguities arise. For example, if the cross flow at the outer edge of the boundary layer becomes slightly negative but remains positive in the rest of the boundary layer, the value of g' will suddenly change sign from one station to the next. This introduces some discontinuity in the flow field since as w_e goes through zero, the value of g' becomes infinite at some net point between the two calculation stations. To avoid this problem, the transformation needs to be changed slightly and the cross-flow velocity w normalized by some reference velocity which does not change sign.

3. A very important study that needs to be conducted involves the procedure with which the calculations are advanced in the spanwise direction. In the present program, a special solution at the root station is obtained prior to calculating the boundary layers on consecutive spanwise stations. At each spanwise station the solution starts with an initial profile and proceeds along the chord until w_e becomes negative. At that point, the program proceeds to the next spanwise station and initiates the calculation at the leading edge and so on. With this procedure the wing is covered from the root to the tip. It should be noted that region I is defined to be the region where w_e is positive. The calculations in region II (this corresponds to the region where w_e is negative) start from the wing tip. The same approximate boundary-layer equations are solved as for the wing-root section to generate the initial conditions along the chord at the wing tip. The rest of the calculation procedure is identical to region I except that now marching is in the inboard direction as the boundary layer is calculated in consecutive spanwise stations all the way to the wing root.

This procedure of marching back and forth requires further study. If there is another region where the cross-flow velocity w_e changes sign, proper logic must be incorporated in the computer program.

An alternative procedure to define separate regions can be utilized by the appearance of negative cross-flow velocity. In such cases, a procedure similar to the present marching procedure can be used. The proper marching procedure requires an extensive and careful study since the locus of streamlines is unknown a priori on complex geometries. An efficient method can only be found by making the actual calculations and changing and testing the logic as required.

REFERENCES

1. Bushnell, Dennis M.; and Beckwith, Ivan E.: Calculation of Nonequilibrium Hypersonic Turbulent Boundary Layers and Comparisons With Experimental Data. AIAA J., vol. 8, no. 8, Aug. 1970, pp. 1462-1469.

2. Harris, Julius E.: Numerical Solution of the Equations for Compressible Laminar, Transitional, and Turbulent Boundary Layers and Comparisons With Experimental data. NASA TR R-368, 1971.

3. Cebeci, Tuncer: Calculation of Three-Dimensional Boundary Layers. I. Swept Infinite Cylinders and Small Cross Flow. AIAA J., vol. 12, no. 6, June 1974, pp. 779-786.

4. Cebeci, Tuncer: A General Method for Calculating Three-Dimensional Incompressible Laminar and Turbulent Boundary Layers. Rep. No. MDC J6517 (Contract No. N00014-72-C-0111), McDonnell Douglas Corp., Mar. 1974. (Available from DDC as AD 779 616.)

5. Keller, Herbert B.; and Cebeci, Tuncer: Accurate Numerical Method for Boundary Layer Flows. I. Two Dimensional Laminar Flows. Proceedings of the Second International Conference on Numerical Methods in Fluid Dynamics. Volume 8 of Lecture Notes in Physics, Maurice Holt, ed., Springer-Verlag, 1971, pp. 92-100.

6. Keller, Herbert B.; and Cebeci, Tuncer: Accurate Numerical Methods for Boundary-Layer Flows. II: Two-Dimensional Turbulent Flows. AIAA J., vol. 10, no. 9, Sept. 1972, pp. 1193-1199.

7. Squire, L. C.: The Three-Dimensional Boundary-Layer Equations and Some Power Series Solutions. R. & M. No. 3006, British A.R.C., 1957.

8. Hansen, Arthur G.: Compressible, Three-Dimensional, Laminar Boundary Layers – A Survey of Current Methods of Analysis. Douglas Paper 3105, Douglas Aircraft Co., Inc., Sept. 28, 1964.

9. Method for Predicting the Pressure Distribution on Swept Wings With Subsonic Attached Flow. Transonic Data Mem. 6312, Roy. Aeronaut. Soc. (London), Dec. 1963.

10. Nash, J. F.; and Scruggs, R. M.: Three-Dimensional Compressible Boundary-Layer Computations for a Finite Swept Wing. NASA CR-112158, [1972].

11. Cebeci, Tuncer; and Smith, A. M. O.: Analysis of Turbulent Boundary Layers. Academic Press, Inc., 1974.

12. Bradshaw, P.: Calculation of Three-Dimensional Turbulent Boundary Layers. J. Fluid Mech., vol. 46, pt. 3, Apr. 13, 1971, pp. 417-445.

13. Donaldson, Coleman duP.; and Sullivan, Roger D.: An Invariant Second-Order Closure Model of the Compressible Turbulent Boundary Layer on a Flat Plate. Contract No. NASW-2224, Aeronaut. Res. Assoc. Princeton, Inc., June 1972. (Available as NASA CR-128172.)

14. Hanjalić, K.; and Launder, B. E.: A Reynolds Stress Model of Turbulence and Its Application to Thin Shear Flows. J. Fluid Mech., vol. 52, pt. 4, Apr. 25, 1972, pp. 609-638.

15. Bradshaw, P.: The Understanding and Prediction of Turbulent Flow. J. Roy. Aeronaut. Soc., vol. 76, no. 739, 1972, pp. 403-418.

16. Bradshaw, P.: Anomalous Effects of Pressure Gradient on Supersonic Turbulent Boundary Layers. Rep. No. 72-21, Aeronaut. Dep., Imperial College Sci. & Technol., Nov. 1972.

17. Keller, Herbert B.: A New Difference Scheme for Parabolic Problems. Numerical Solution of Partial Differential Equations – II, Bert Hubbard, ed., Academic Press, Inc., 1971, pp. 327-350.

18. Isaacson, Eugene; and Keller, Herbert Bishop: Analysis of Numerical Methods. John Wiley & Sons, Inc., c.1966.

19. East, L. F.; and Hoxey, R. P.: Low-Speed Three-Dimensional Turbulent Boundary-Layer Data. Parts 1 and 2. R. & M. No. 3653, British A.R.C., 1971.

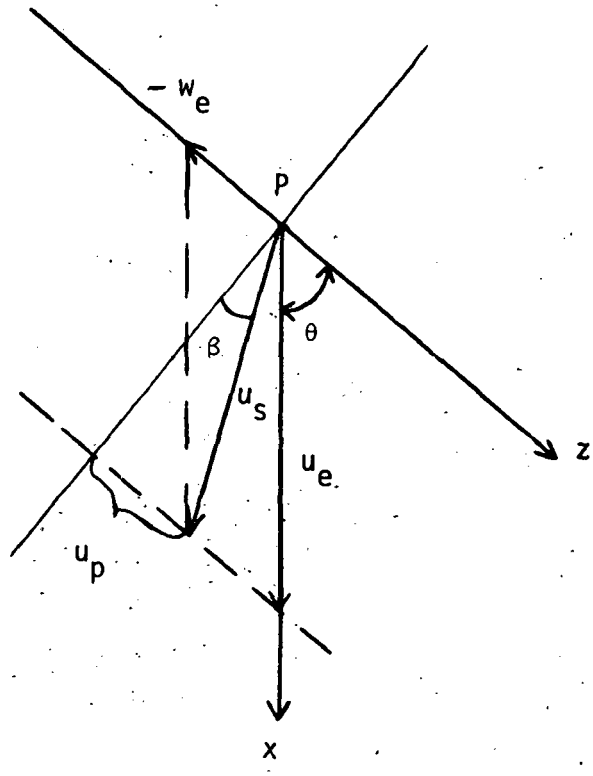

Figure 1.- Velocity vector in the tangent plane at a point P on the wing.

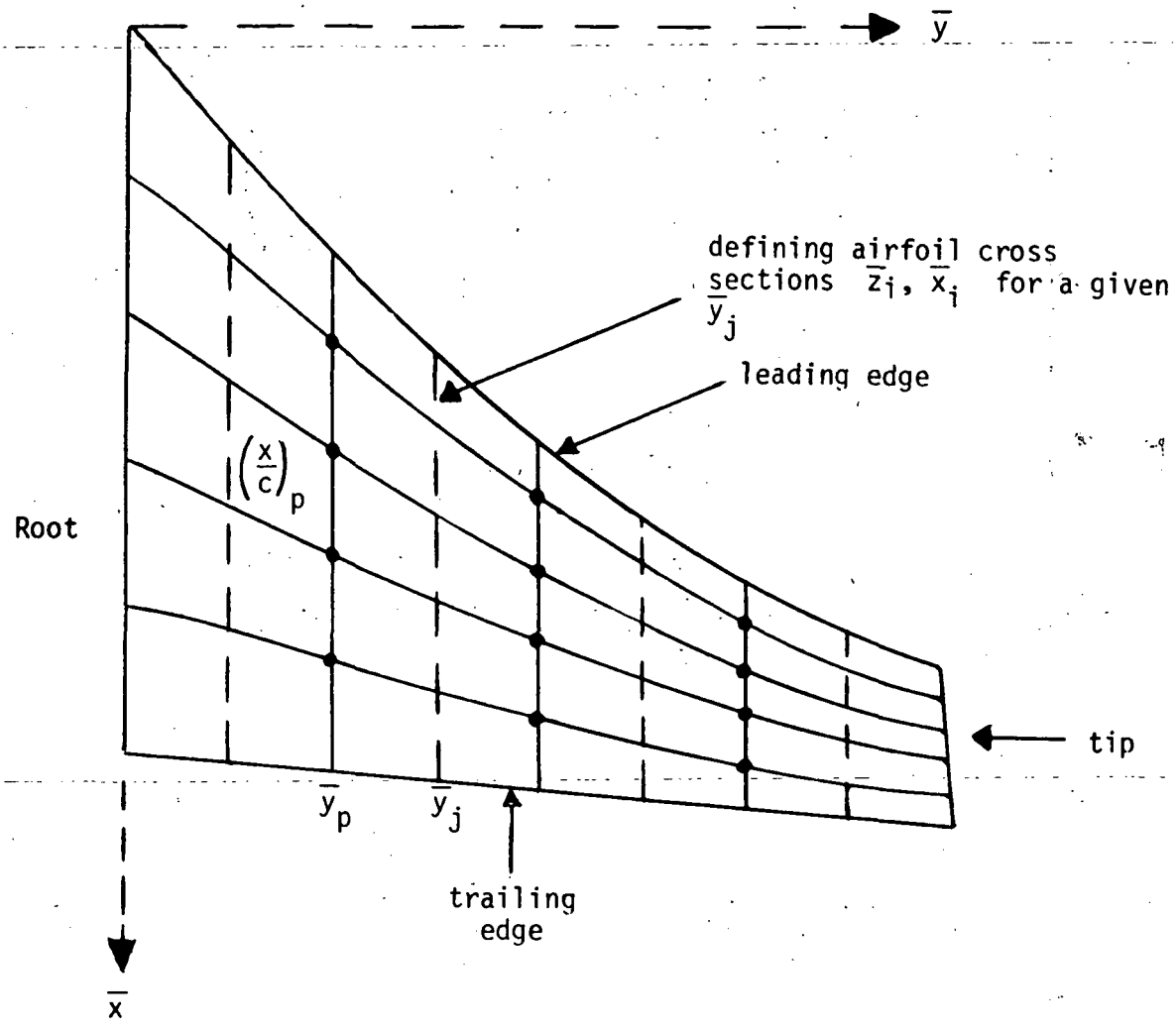

Figure 2.- Schematic of typical wing.

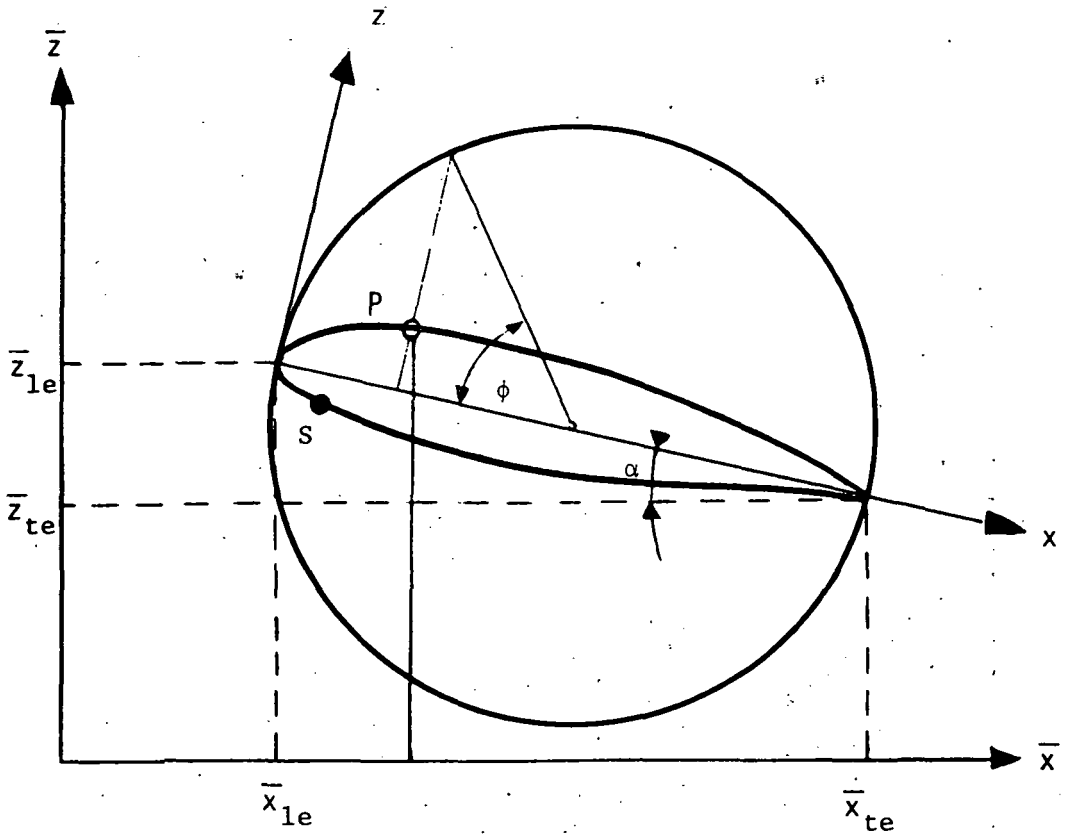

Figure 3.- Notation for the airfoil section for a given $\bar{y}_j$.

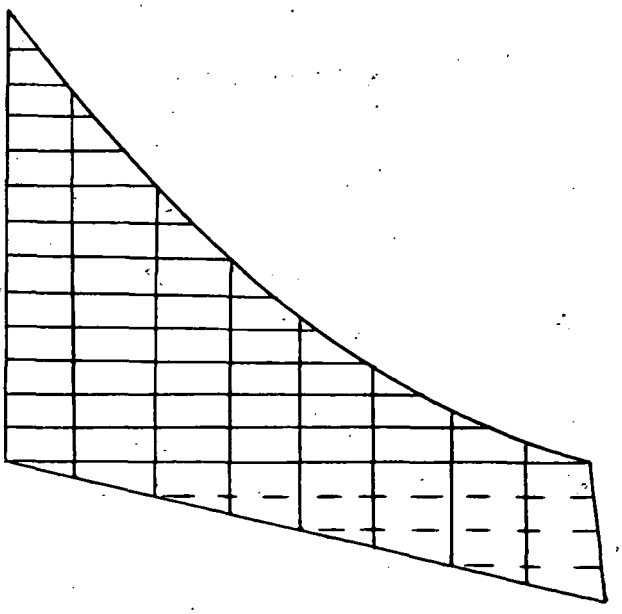

Figure 4.- An orthogonal system for the wing.

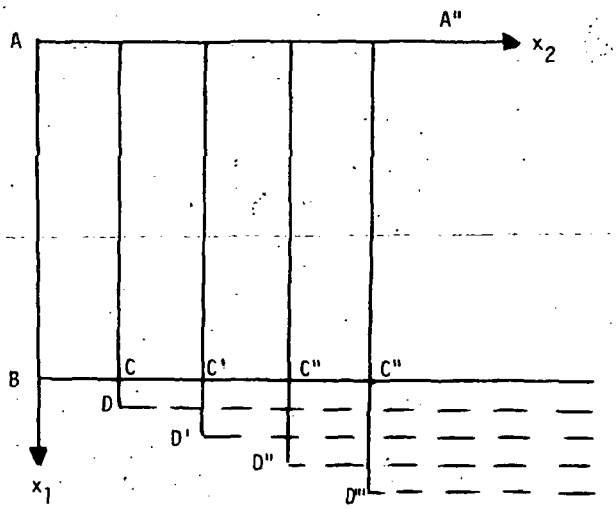

Figure 5.- Wing in the x_1 and x_2 plane.

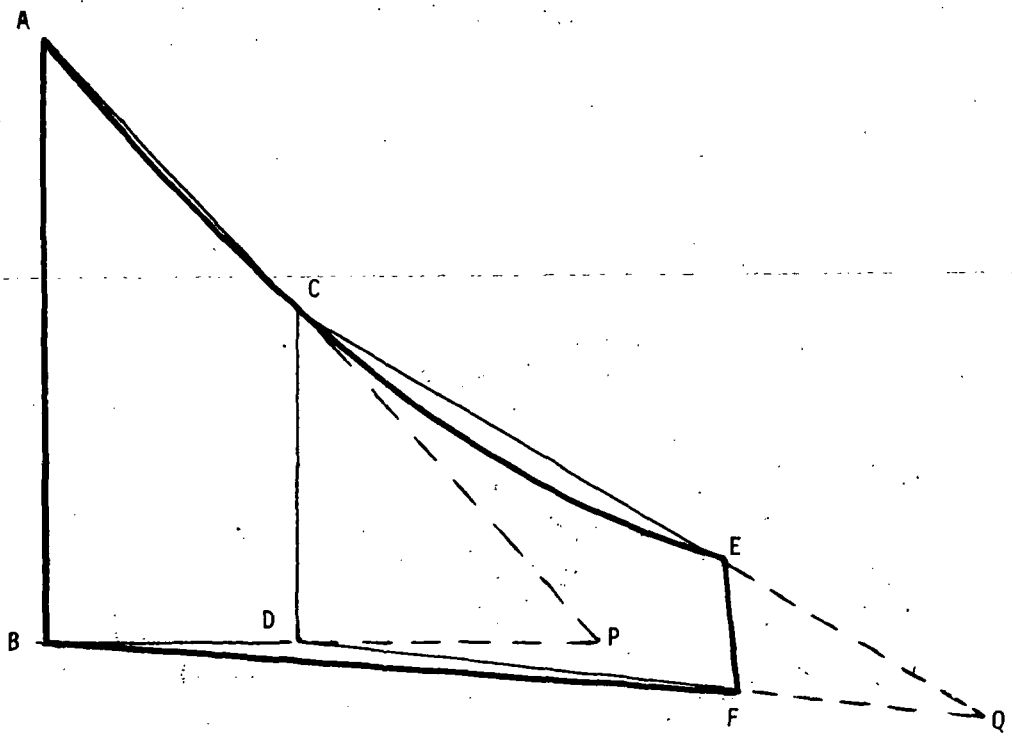

Figure 6.- Representation of the wing by conical sections.

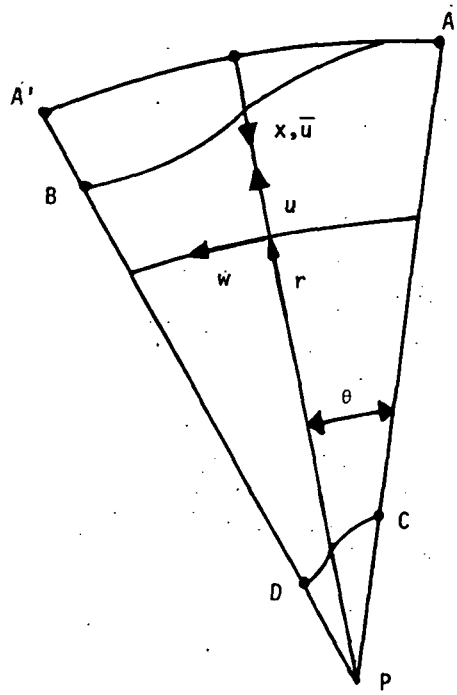

Figure 7.- Notation for conical section ABDC and the coordinate system in the developed plane.

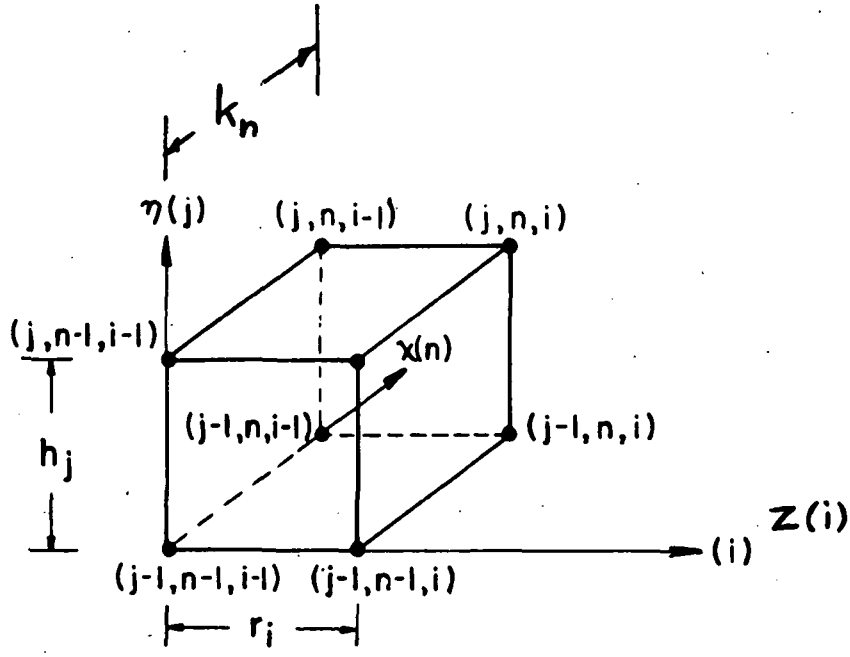

Figure 8.- Net cube for the difference equations for three-dimensional flows.

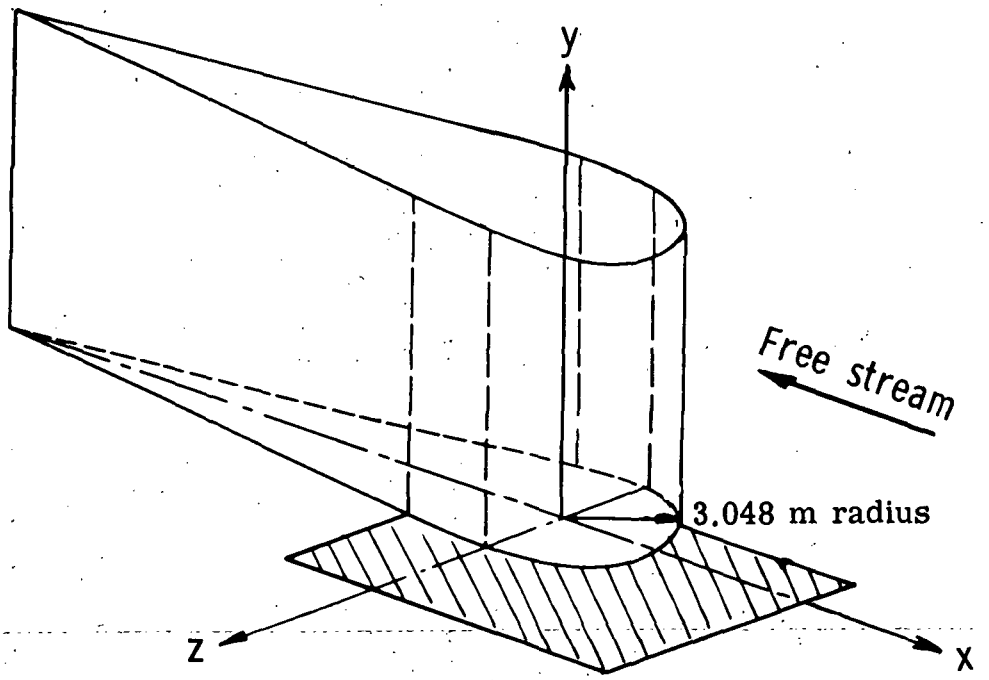

(a) Schematic drawing of test setup.

Figure 9.- Comparisons of numerical results with experimental data.

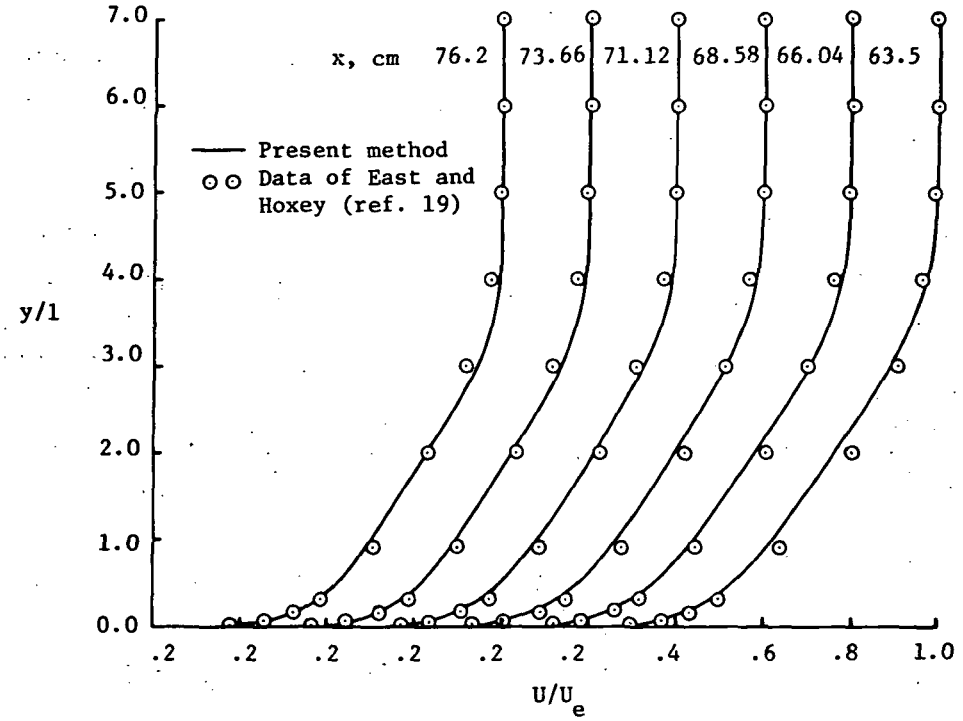

(b) z = 5.09 cm (1 = 2.54 cm).

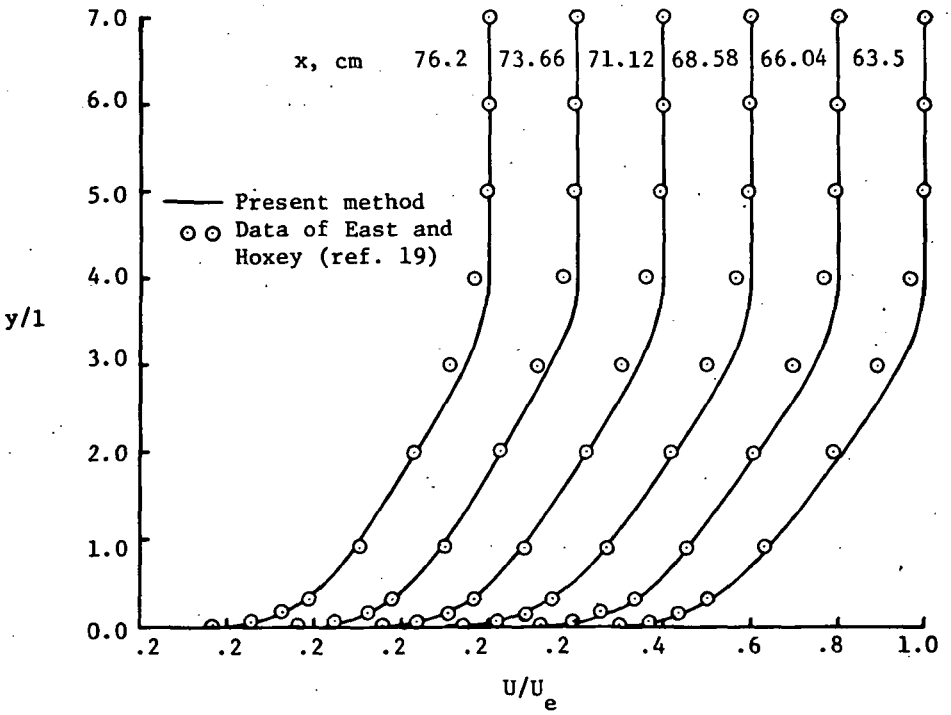

(c) z = 7.62 cm (1 = 2.54 cm).

Figure 9.- Concluded.

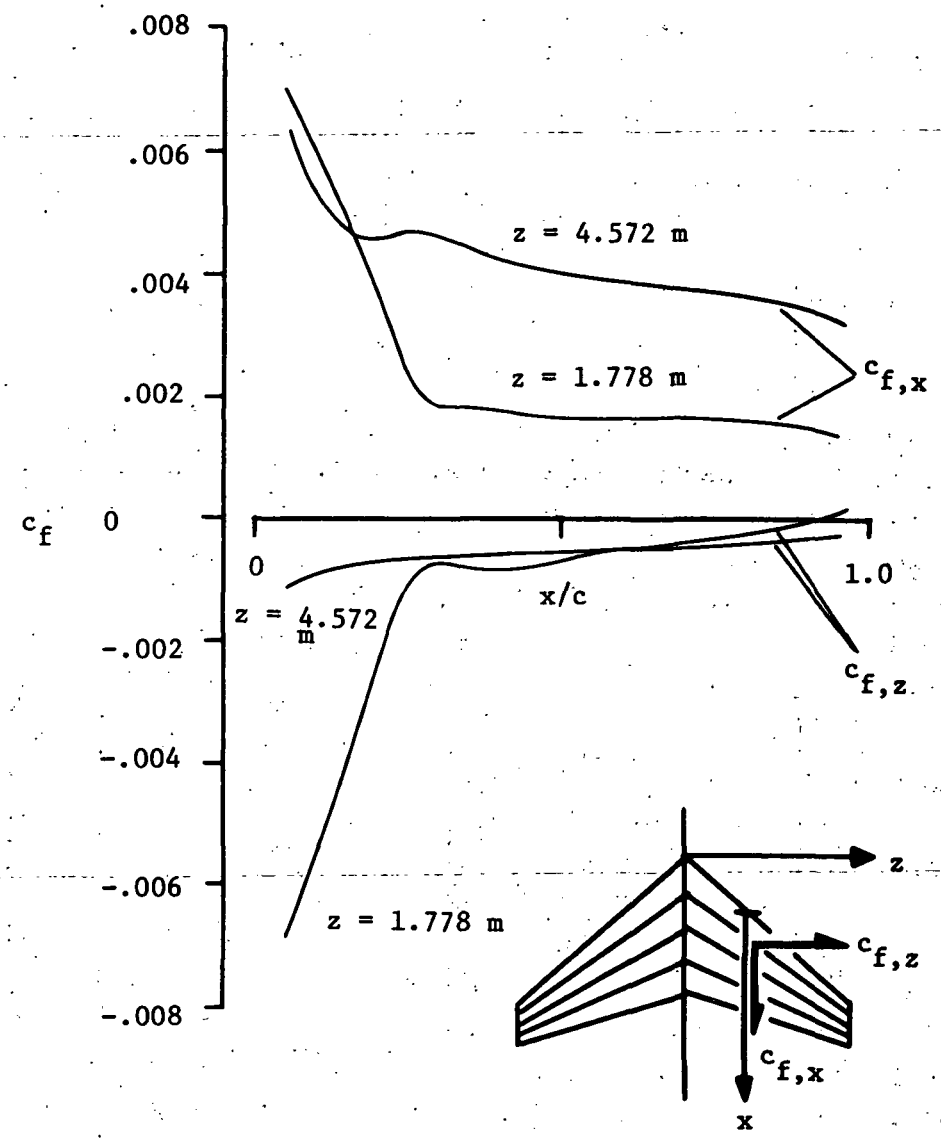

Figure 10.- Calculated skin-friction coefficients for upper surface of a swept wing. Schematic of planform illustrates notation and does not represent calculated wing.